Silver-based crystalline nanoparticles, microbially fabricated

Tanja Klaus*, Ralph Joerger, Eva Olsson, and Claes-Göran Granqvist

Department of Materials Science, The Ångström Laboratory, Uppsala University, P. O. Box 534, SE-751 21 Uppsala, Sweden.

Edited by Frank H. Stillinger, Bell Laboratories, Lucent Technologies, Murray Hill, NJ, and approved September 21, 1999 (received for review May 20, 1999)

One mechanism of silver resistance in microorganisms is accumulation of the metal ions in the cell. Here, we report on the phenomenon of biosynthesis of silver-based single crystals with well-defined compositions and shapes, such as equilateral triangles and hexagons, in *Pseudomonas stutzeri* AG259. The crystals were up to 200 nm in size and were often located at the cell poles. Transmission electron microscopy, quantitative energy-dispersive x-ray analysis, and electron diffraction established that the crystals comprise at least three different types, found both in whole cells and thin sections. These Ag-containing crystals are embedded in the organic matrix of the bacteria. Their possible potential as organic-metal composites in thin film and surface coating technology is discussed.

There is much current interest in metal–microbial interactions, especially concerning biochemical, toxicological, environmental, and industrial aspects (1). Microbial resistance against heavy metal ions such as Fe, Co, Ni, Cu, Zn, As, Cd, Hg, Pb, or U has been explored for bioleaching processes of ores (2–4) and for biological metal recovery systems (5–9). Much less is known about resistance against the noble metals (10, 11), although it has been stated that gold can serve as a slow acting drug in rheumatology (10). Silver is highly toxic to most microbial cells and can be used as a biocide or antimicrobial agent (12). Nevertheless, it has been reported that several bacterial strains are silver-resistant (13, 14) and may even accumulate silver at the cell wall to as much as 25% of the dry weight biomass, thus suggesting their use for industrial recovery of silver from ore materials (13).

Here, we describe the biological synthesis of silver-based crystals with sizes up to 200 nm in the periplasmic space of *Pseudomonas stutzeri* AG259, a bacterial strain that was originally isolated from a silver mine (15).

Materials and Methods

Bacterial Strain and Growth Conditions. *Pseudomonas stutzeri* AG259 was kindly obtained from J. T. Trevors (University of Guelph, ON, Canada). The silver-resistant *P. stutzeri* AG259 strain was maintained in Lennox L (LB) broth. Bacteria were grown on Lennox L (LB) agar substrate, containing 50 mM $AgNO_3$, at 30°C for 48 hr in the dark.

Transmission Electron Microscopy (TEM), Energy Dispersive X-Ray Analysis (EDX), and Electron Diffraction. Growing cells were harvested and fixed for 2 hr in 2.5% glutaraldehyde in distilled water. After fixation at room temperature, the cells were sedimented (1,500 × *g*, 10 min) and washed three times in distilled water. The pellet was not postfixed. For the preparation of thin sections, the pellet was dehydrated with 30, 50, 70, and 95% (vol/vol, aq.) ethanol for 15 min each, followed by absolute ethanol. Embedding was in absolute ethanol/Agar 100 epoxy resin (Agar Scientific) at a ratio of 1:1 overnight at room temperature. Polymerization at 60°C was carried out in 100% Agar 100 epoxy resin for 2 days. Ultrathin sections were cut on an ultramicrotome, and some of the sections were slightly stained with uranyl acetate and lead citrate. Sections were mounted on Formvar-coated Ti grids. Micrographs were taken with a 2000FX II TEM instrument (JEOL), operating at 200 kV; EDX spectra were acquired with a Link AN10,000 system attached to the TEM. The spectra were evaluated using the RTS/2-FLS program taking into account the sensitivity factors for the different elements (*k*-factor correction). The beam spot sizes that were used depended on the size of the particles. They were between about 20 and 50 nm. We took care not to include more than one particle in the beam. Microdiffraction was used for careful orientation of the crystals, and selected area diffraction patterns were recorded for identification of crystal structures.

Results and Discussion

We used TEM of the silver-resistant bacterial strain *P. stutzeri* AG259, cultured in the presence of high concentrations of silver salts (50 mM $AgNO_3$), to show that the cells can accumulate silver in large quantities. The extent and appearance of the Ag deposition in the periplasm of the bacteria is illustrated in Fig. 1, which gives a representative overview of thin sections of a cell culture prepared by removing active cells grown in the dark from an agar plate. The sections demonstrated that most cells exhibited numerous silver-containing particles.

However, in contrast to many other reports of metal-resistant bacteria, for which efflux of toxic ions is the main detoxification mechanism (16, 17), the majority of the accumulated silver here is deposited as particles in vacuole-like granules between the outer membrane and the plasma membrane. Particles have linear extents from a few to 200 nm or more. Previous studies have shown that the Ag resistance in *P. stutzeri* AG259 is associated with metal accumulation (14). The sizes of the deposits described in this earlier publication were rather small and ranged from 35 to 46 nm. The difference in our results may be caused by different cell growth and metal incubation conditions. The authors of ref. 14 suggested that, according to EDX analysis of whole cells, the deposits were most likely silver sulfide.

Fig. 2 illustrates selected examples of whole cells with large accumulated particles that have crystallized in distinct shapes, such as equilateral triangles and hexagons, as observed in projection. Frequently, the cell poles serve as preferred accumulation sites (Fig. 2*a*), but other locations are also possible (Fig. 2 *b* and *c*). Large particles with distinct shapes as well as small colloidal particles can be found all over the cell wall.

At least three different crystal types could be analyzed by using TEM, EDX, and electron diffraction, as shown in Fig. 3. The different types were found in whole cells as well as in thin sections. In our studies, most of the silver was deposited in elemental form; Fig. 3*a* illustrates an almost triangular silver crystal from a thin-sectioned sample, its diffraction pattern showing diffraction spots corresponding the [111] and [200] planes of the fcc structure of elemental silver. The corresponding

This paper was submitted directly (Track II) to the PNAS office.

Abbreviations: TEM, transmission electron microscopy; EDX, energy-dispersive x-ray analysis.

*To whom reprint requests should be addressed. E-mail: Tanja.Klaus@angstrom.uu.se.

The publication costs of this article were defrayed in part by page charge payment. This article must therefore be hereby marked "*advertisement*" in accordance with 18 U.S.C. §1734 solely to indicate this fact.

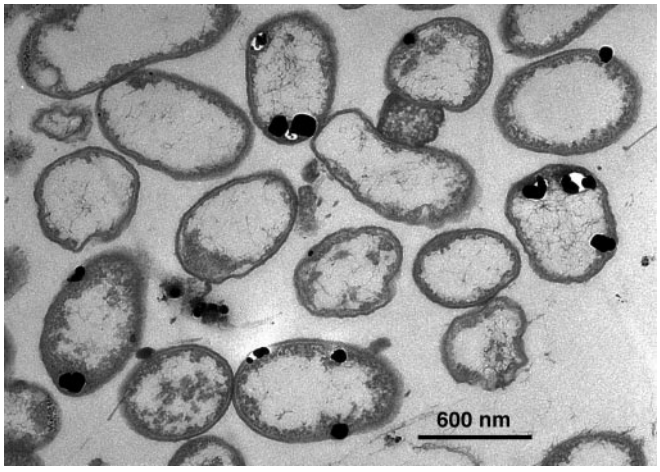

Fig. 1. TEM of a thin section of *P. stutzeri* AG259 cells. Large crystalline Ag^0 and Ag_2S particles are deposited between the cell wall and the plasma membrane.

EDX spectrum indicates a silver content of about 91 atom %. Minor amounts of other elements, especially chlorine and sodium, may result from the surrounding organic material. The titanium signal is caused by the Ti grid that was used for the TEM analysis.

A small number of the particles crystallize as silver sulfide (apparent in Fig. 3*b*). The EDX spectrum shows Ag and S in the proportion 2:1, thus suggesting the formula Ag_2S. The electron diffraction pattern displays diffraction spots corresponding to the [030] and the [$\bar{1}\bar{2}$4] planes, indicating an orientation close to the ⟨401⟩ zone axis of acanthite, a monoclinic crystalline α-form of Ag_2S known to be stable below 173°C (information available at website http://209.51.193.54/minerals/sulfides/acanthit/acanthit.htm).

The large crystal in the middle of Fig. 3*c* represents a third type of crystal embedded in a whole cell and having an as-yet-undetermined structure. The EDX spectrum shows mainly Ag (77 atom %) and only minor amounts of other elements with P (8.7 atom %) and Cl (7.4 atom %) being the largest. EDX spectra acquired from thin sections reached values typical for the elemental Ag crystal type (about 90 atom %). These results may be taken as evidence of the crystal being of elemental silver, but the electron diffraction pattern rules out this identification. A diffraction pattern can be identified by taking the ratio between the two shortest vectors, each drawn from the central spot to a diffracted spot, and the angle between them. In this particular case, the angle between the shortest vectors was 64°. This angle differs significantly from 70.5°, which would be expected for crystalline Ag. Furthermore, the interplanar distances do not exactly match the ones for crystalline silver, as can be seen from the diffraction rings of a thin gold layer, which was sputtered onto the sample for calibration purposes. It remains a possibility that the third type of crystals contains H, C, N and/or O. These elements either cannot be detected by EDX (H), or the detectability and accuracy of EDX for these elements may be relatively poor.

The resistance mechanisms that enable *P. stutzeri* AG259 to grow in an extreme silver rich—and for other bacterial strains toxic—environment are still poorly understood. However, microbial resistance mechanisms against toxic silver concentrations in other bacterial strains currently under investigation are the cellular efflux pumping systems that protect the cytoplasm against toxic concentrations and the small periplasmic silver-binding proteins that bind silver specifically at the cell surface (18, 19). The results shown in the present work may be interpreted on the premise that the resistance to silver in *P. stutzeri* AG259 can involve formation and accumulation of silver precipitates outside the cytoplasmic membrane, possibly accompanied by metal efflux and metal binding. The formation of acanthite crystals may then be caused by a facile reaction of the silver particles with H_2S gas, which was reportedly (14) produced by *P. stutzeri* uniquely among the pseudomonads.

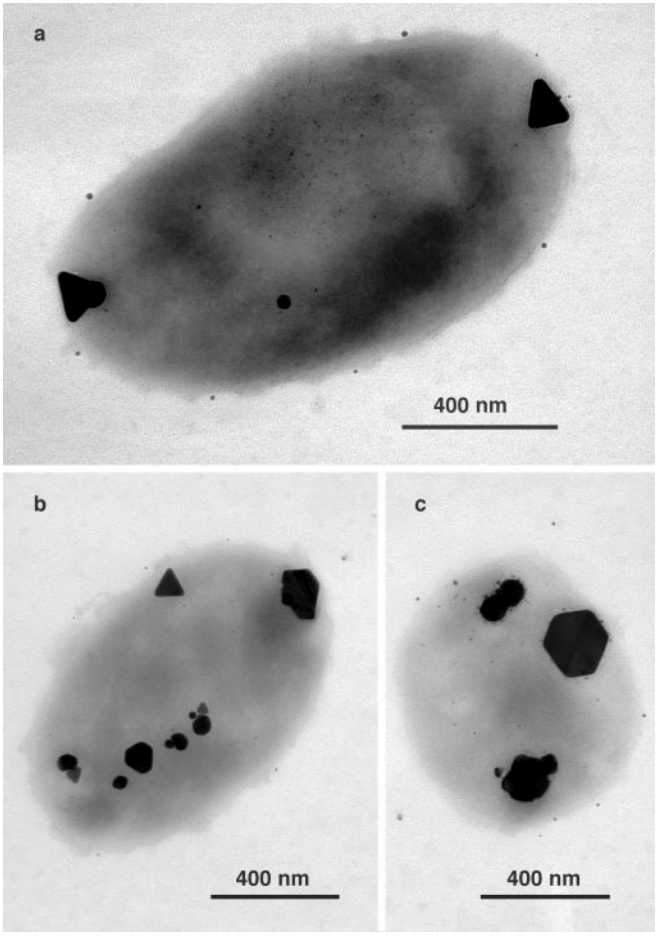

Fig. 2. A variety of crystal typologies; i.e., different morphologies, sizes, and chemical compositions can be produced by *P. stutzeri* AG259. (*a*) Whole, uncontrasted cell grown on Ag^+-containing environment with large, triangular, Ag-containing particles at both poles; an accumulation of smaller Ag-containing particles can be found all over the cell. (*b* and *c*) Triangular, hexagonal, and spheroidal Ag-containing nanoparticles accumulated at different cellular binding sites.

The synthesis of materials with dimensions on the nanometer scale is a continuing challenge in materials science and in microelectronics (20). Direct biosynthesis to make microelectronic devices may become feasible (21). The present study indicates avenues toward the preparation of nanostructured materials that incorporate silver-based crystalline particles with defined structural, compositional, and morphological properties. Other techniques to prepare this type of material (20, 22), such as gas condensation and irradiation by ultraviolet or γ radiation, are usually associated with low production rate and high expense. Large-scale production of silver-containing materials by chemical deposition or solution reduction usually produces particles larger than a few micrometers. We expect that the tolerance of *P. stutzeri* AG259 to silver ions and the formation of the silver-based crystallites each depend on physical and chemical growth parameters. Particle size and morphology-controlling parameters can depend on, e.g., growth conditions such as pH,

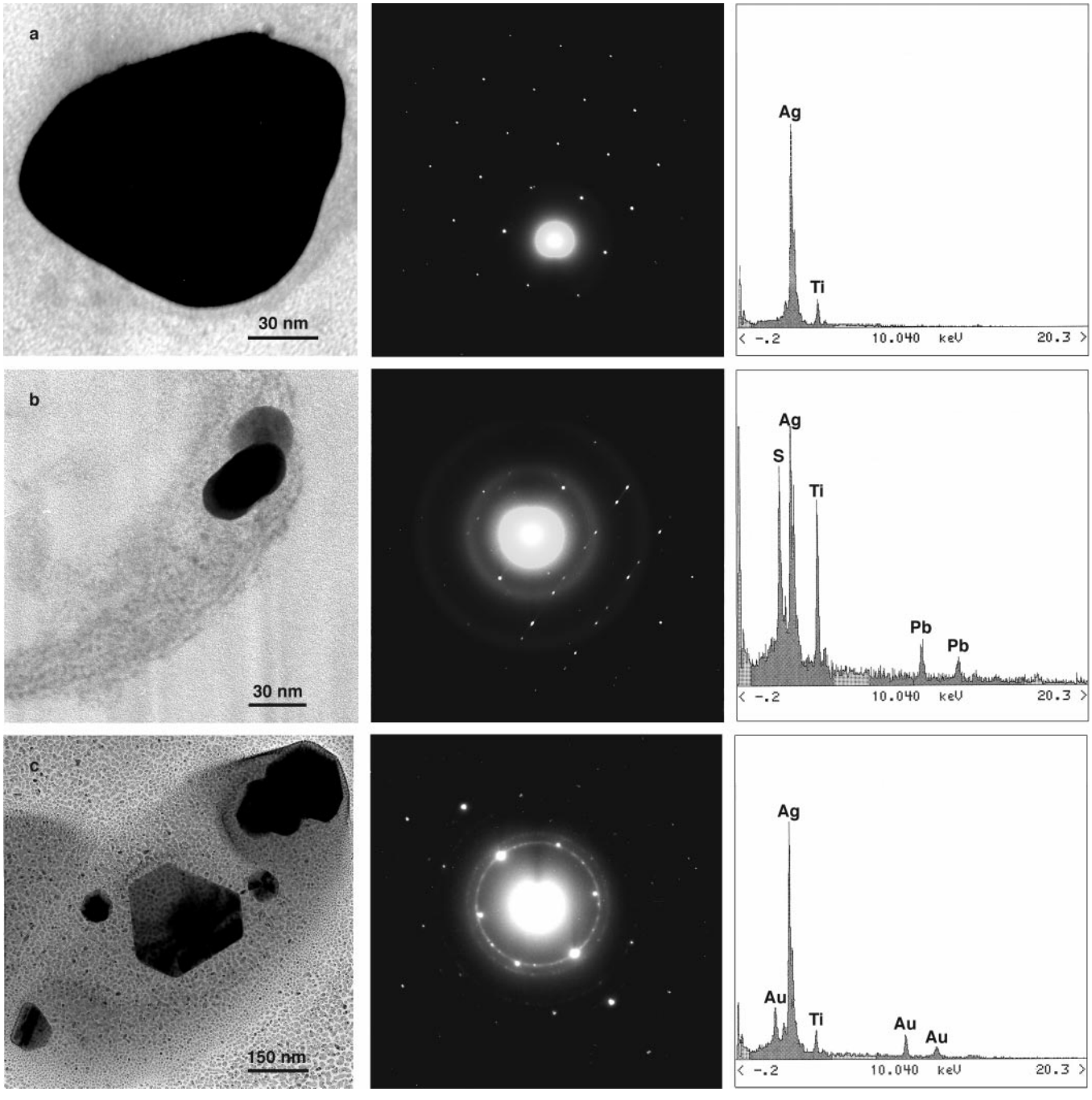

Fig. 3. Crystal structure analysis. (*a*) Regularly shaped nanocrystalline Ag particle taken from a thin, unstained section of a *P. stutzeri* AG259 cell, with a corresponding EDX spectrum (*Right*) and its electron diffraction pattern (*Center*) indicating elemental crystalline silver. (*b*) Second crystal type embedded in the periplasmic space of the cell. EDX spectrum and electron diffraction indicate monoclinic Ag_2S. (*c*) A third type of crystal taken from a whole cell. The crystal structure is not yet clear. The electron diffraction pattern is not consistent with the pattern of elemental silver, whereas the EDX spectrum shows only Ag in considerable amounts.

incubation time, growth in light or dark, and/or the composition of the culture medium. However, direct control of the properties of bacterially produced Ag particles through cultivation conditions will be a topic of future investigations.

Metal-insulator composite materials have interesting optical and electrical properties that favor their application in microelectronics, for example, or as functional optical thin-film coatings. The possibility of synthesizing metal particles directly in an organic matrix points toward new uses of metal-containing bacteria as precursors in thin film and surface coating technology, for which a composite or cermet structure can yield controlled optical, electrical, and other properties. Thin-film coatings based on Ag particles biosynthesized as discussed above showed distinct wavelength-selective optical properties. A characteristic optical absorption edge around a wavelength of about 1 μm was adjustable both in spectral position and in steepness by the metal concentration and a special temperature treatment. Further work is required for detailed elaboration.

The authors thank Prof. C. Kurland for hosting the biological part of the project in the Biomedical Center at Uppsala University, and Prof. J. T.

Trevors at the University of Guelph, ON, Canada, for supplying the *Pseudomonas stutzeri* strain. This work was financially supported by the European Union (contract nos. ERBFMBICT961210 and ERBFMBICT983046) and by The Ångström Solar Center at Uppsala University.

1. Beveridge, T. J., Hughes, M. N., Lee, H., Leung, K. T., Poole, R. K., Savvaidis, I., Silver, S. & Trevors, J. T. (1997) *Adv. Microb. Physiol.* **38,** 177–243.
2. Dopson, M. & Lindstrom, E. B. (1999) *Appl. Environ. Microbiol.* **65,** 36–40.
3. Bacelar-Nicolau, P. & Johnson, D. B. (1999) *Appl. Environ. Microbiol.* **65,** 585–590.
4. Lundgren, D. G & Silver, M. (1980) *Annu. Rev. Microbiol.* **34,** 263–283.
5. White, C., Sayer, J. A. & Gadd, G. M. (1997) *FEMS Microbiol. Rev.* **20,** 503–516.
6. Nies, D. H. (1992) *Plasmid* **27,** 17–28.
7. White, C., Sharman, A. K. & Gadd, G. M. (1998) *Nat. Biotechnol.* **16,** 572–575.
8. Misra, T. K. (1992) *Plasmid* **27,** 4–16.
9. Jeong, B. C., Hawes, C., Bonthrone, K. M. & Macaskie, L. E. (1997) *Microbiology* **143,** 2497–2507.
10. Rhodes, M. D., Sadler, P. J., Scawen, M. D. & Silver, S. (1992) *J. Inorg. Biochem.* **46,** 129–142.
11. Slawson, R. M., Lee, H. & Trevors, J. T. (1990) *Biol. Met.* **3,** 151–154.
12. Slawson, R. M., Van Dyke, M. I., Lee, H. & Trevors, J. T. (1992) *Plasmid* **27,** 72–79.
13. Pooley, F. D. (1982) *Nature (London)* **296,** 642–643.
14. Slawson, R. M., Trevors, J. T. & Lee, H. (1992) *Arch. Microbiol.* **158,** 398–404.
15. Haefeli, C., Franklin, C. & Hardy, K. (1984) *J. Bacteriol.* **158,** 389–392.
16. Silver, S. & Phung, L. T. (1996) *Annu. Rev. Microbiol.* **50,** 753–789.
17. Gupta, A., Matsui, K., Lo, J. F. & Silver, S. (1999) *Nat. Med.* **5,** 183–188.
18. Li, X. Z., Nikaido, H. & Williams, K. E. (1997) *J. Bacteriol.* **179,** 6127–6132.
19. Gupta, A. & Silver, S. (1998) *Nat. Biotechnol.* **16,** 888.
20. Li, Y., Duan, X., Qian, Y., Yang, L. & Liao, H. (1999) *J. Colloid. Interface Sci.* **209,** 347.
21. Dameron, C. T., Reese, R. N., Mehra, R. K., Kortan, A. R., Carroll, P. J., Steigerwald, M. L., Brus, L. E. & Winge, D. R. (1989) *Nature (London)* **338,** 596–597.
22. Kreibig, U. & Vollmer, M. (1995) in *Optical Properties of Metal Clusters*, eds. Gonser, U., Osgood, R. M., Panish, M. B. & Sakaki, H. (Springer, Berlin), pp. 207–234.